Supplemental Tables and Figures

Table S1. Comparison of genetic composition of VRC-PG05 with that of VRC-PG04 isolated from the same IAVI Donor #74. Related to Figure 1.

Antibody	Donor	IGHV	IGHV mutation frequency	CDRH3 length (amino acid)	IGKV	IGKV mutation frequency	CDRL3 length (amino acids)
VRC-PG05	IAVI 74	3-7*01	27/288 (9%)	17	4-1*01	17/282 (6%)	8
VRC-PG04	IAVI 74	1-2*02	86/288 (30%)	14	3-20*01	51/267 (19%)	5
VRC-PG04b	IAVI 74	1-2*02	85/288 (30%)	14	3-20*01	50/267 (19%)	5

Table S2. Neutralization IC_{50} values of VRC-PG05 against 208 HIV-1 Env pseudoviruses. Related to Figure 1.

Virus	Clade	IC50 (µg/ml)	Virus	Clade	IC50 (µg/ml)	Virus	Clade	IC50 (µg/ml)	Virus	Clade	IC50 (µg/ml)
0260.v5.c36	A	>50	R2184.c4	AE	43.000	SS1196.01	B	>50	DU123.06	C	>50
0330.v4.c3	A	>50	R3265.c6	AE	>50	THRO.18	B	>50	DU151.02	C	0.577
0439.v5.c1	A	>50	TH023.6	AE	0.1750	TRJO.58	B	>50	DU156.12	C	>50
3365.v2.c20	A	3.710	TH966.8	AE	34.300	TRO.11	B	>50	DU172.17	C	>50
3415.v1.c1	A	>50	TH976.17	AE	>50	WITO.33	B	>50	DU422.01	C	5.990
3718.v3.c11	A	>50	235-47	AG	>50	X2278.C2.B6	B	>50	MW965.26	C	>50
398-F1_F6_20	A	>50	242-14	AG	>50	YU2.DG	B	>50	SO18.18	C	>50
BB201.B42	A	>50	263-8	AG	>50	BJOX002000.03.2	BC	>50	TV1.29	C	>50
BB539.2B13	A	>50	269-12	AG	>50	CH038.12	BC	17.80	TZA125.17	C	>50
BG505.W6M.C2	A	>50	271-11	AG	>50	CH070.1	BC	0.341	TZBD.02	C	17.100
BI369.9A	A	>50	928-28	AG	0.875	CH117.4	BC	>50	ZA012.29	C	>50
BS208.B1	A	>50	DJ263.8	AG	>50	CH119.10	BC	>50	ZM106.9	C	>50
KER2008.12	A	>50	T250-4	AG	>50	CH181.12	BC	>50	ZM109.4	C	0.520
KER2018.11	A	>50	T251-18	AG	>50	CNE15	BC	>50	ZM135.10a	C	>50
KNH1209.18	A	>50	T253-11	AG	>50	CNE19	BC	>50	ZM176.66	C	>50
MB201.A1	A	>50	T255-34	AG	0.566	CNE20	BC	>50	ZM197.7	C	>50
MB539.2B7	A	>50	T257-31	AG	>50	CNE21	BC	>50	ZM214.15	C	>50
MI369.A5	A	>50	T266-60	AG	>50	CNE40	BC	>50	ZM215.8	C	>50
MS208.A1	A	>50	T278-50	AG	>50	CNE7	BC	0.054	ZM233.6	C	>50
Q23.17	A	>50	T280-5	AG	>50	286.36	C	>50	ZM249.1	C	>50
Q259.17	A	>50	T33-7	AG	>50	288.38	C	>50	ZM53.12	C	0.171
Q769.d22	A	0.724	3988.25	B	12.6000	0013095-2.11	C	>50	ZM55.28a	C	>50
Q769.h5	A	0.016	5768.04	B	>50	001428-2.42	C	0.324	3326.V4.C3	CD	>50
Q842.d12	A	>50	6101.10	B	43.5000	0077_V1.C16	C	0.051	3337.V2.C6	CD	2.780
QH209.14M.A2	A	0.298	6535.3	B	>50	00836-2.5	C	>50	3817.v2.c59	CD	>50
RW020.2	A	>50	7165.18	B	>50	0921.V2.C14	C	0.111	191821.E6.1	D	>50
UG037.8	A	>50	45_01dG5	B	>50	16055-2.3	C	>50	231965.c1	D	>50
246-F3.C10.2	AC	0.059	89.6	B	>50	16845-2.22	C	>50	247-23	D	19.000
3301.V1.C24	AC	>50	AC10.29	B	0.019	16936-2.21	C	>50	3016.v5.c45	D	7.120
3589.V1.C4	AC	>50	ADA	B	29.400	25710-2.43	C	>50	57128.vrc15	D	>50
6540.v4.c1	AC	>50	Bal.01	B	0.642	25711-2.4	C	7.620	6405.v4.c34	D	>50
6545.V4.C1	AC	>50	BaL.26	B	0.897	25925-2.22	C	>50	A03349M1.vrc4a	D	>50
0815.V3.C3	ACD	>50	BG1168.01	B	>50	26191-2.48	C	>50	A07412M1.vrc12	D	>50
6095.V1.C10	ACD	0.013	BL01	B	>50	3168.V4.C10	C	0.031	NKU3006.ec1	D	>50
3468.V1.C12	AD	>50	BR07	B	>50	3637.V5.C3	C	>50	UG021.16	D	>50
Q168.a2	AD	>50	BX08.16	B	>50	3873.V1.C24	C	>50	UG024.2	D	>50
Q461.e2	AD	>50	CAAN.A2	B	0.003	426c	C	>50	P0402.c2.11	G	>50
620345.c1	AE	0.336	CNE10	B	>50	6322.V4.C1	C	2.260	P1981.C5.3	G	>50
BJOX009000.02.4	AE	>50	CNE12	B	1.600	6471.V1.C16	C	>50	X1193.c1	G	>50
BJOX010000.06.2	AE	>50	CNE14	B	0.003	6631.V3.C10	C	>50	X1254.c3	G	>50
BJOX025000.01.1	AE	1.950	CNE4	B	>50	6644.V2.C33	C	>50	X1632.S2.B10	G	>50
BJOX028000.10.3	AE	>50	CNE57	B	10.700	6785.V5.C14	C	>50	X2088.c9	G	>50
C1080.c3	AE	45.900	HO86.8	B	1.430	6838.V1.C35	C	1.000	X2131.C1.B5	G	>50
C2101.c1	AE	2.300	HT593.1	B	0.453	96ZM651.02	C	>50	*356272.c02 **	AE	1.420
C3347.c11	AE	3.420	HXB2	B	>50	BR025.9	C	>50	*427299.c12*	AE	>50
C4118.09	AE	2.540	JR-CSF	B	>50	CAP210.E8	C	>50	*703357.c02*	AE	>50
CM244.ec1	AE	>50	JR-FL	B	2.650	CAP244.D3	C	>50	*816763.c02*	AE	12.200
CNE3	AE	0.053	MN.3	B	>50	CAP256.206.C9	C	>50	*254001P00Ra.1*	AE	>50
CNE5	AE	0.026	PVO.04	B	>50	CAP45.G3	C	>50	*254004P00Rc.2*	AE	0.265
CNE55	AE	0.012	QH0515.01	B	>50	Ce1176.A3	C	>50	*254006P00Ra.1*	AE	>50
CNE56	AE	15.000	QH0692.42	B	>50	Ce703010217.B6	C	>50	*40061v03.04b*	AE	>50
CNE59	AE	45.000	REJO.67	B	>50	CNE30	C	>50	*40100v01.09*	AE	>50
CNE8	AE	5.880	RHPA.7	B	>50	CNE31	C	>50	*40363v03.02*	AE	1.680
M02138	AE	0.091	SC422.8	B	>50	CNE53	C	>50	*644039.c01b*	AE	>50
R1166.c1	AE	>50	SF162	B	>50	CNE58	C	0.037	*NP03-C03*	AE	>50

IC50 color code: 0.001-0.01 | 0.01-0.100 | 0.100-1.00 | 1.00-10.0 | 10.0-50.0 | >50.0 (µg/ml)

* Neutralization IC_{50} to 12 clade AE strains (shown in italics) in addition to the standard 208-virus panel are also listed.

Table S3. Statistics on VRC-PG05 neutralization profile based on the extended 220-isolate panel. Related to Figure 1.

Neutralization panel	Number of isolates in panel	Number of sensitive isolates	Neutralization breadth (%)
Neutralization breadth on 208 isolate panel	208	56	26.9
Neutralization breadth on global virus panel	12	3	25.0
Neutralization breadth against tier 2 isolates	154	40	26.0
Neutralization breadth on 35 clade AE isolates	35	20	57.1
Neutralization breadth on glycan N262, glycan N295, and glycan N448 containing isolates	96	26	27.1
Neutralization breadth on glycan N262, glycan N448, and E293 containing isolates	89	51	57.3
Neutralization breadth on 220 isolate panel	220	60	27.3

Table S4. Crystallographic data collection and refinement statistics. Related to Figure 2.

Protein	VRC-PG05-gp120
PDB ID	6BF4
Data collection	
Space group	C2
Cell dimensions	
a, *b*, *c* (Å)	231.4, 89.3, 123.4
α, β, γ (°)	90.0, 119.2, 90.0
Resolution (Å)	50.0-2.38 (2.42-2.38)
R_{sym} or R_{merge}	7.7 (56.1)
R_{pim}	5.8 (34.6)
$I/\delta I$	17.5 (2.0)
$CC_{1/2}$	0.9 (0.7)
Completeness (%)	88.8 (50.4)
Redundancy	3.3 (2.1)
Refinement	
Resolution (Å)	39.85-2.38 (2.41-2.38)
No. reflections	77844 (2207)
R_{work}/ R_{free}	19.4/23.1
No. atoms	
Protein	12053
Ligand/glycans	911
Water	172
B-factors (Å^2)	
Protein	90.7
Ligand/ion	87.8
Water	54.7
r.m.s deviations	
Bond lengths (Å)	0.003
Bond angles (º)	0.67
Ramachandran statistics	
Favored (%)	93.4
Outliers (%)	0.9

*Values in parenthesis denote highest resolution shell.

Table S5. Contributions of glycan and protein to the VRC-PG05 epitope. Related to Figure 3 and 6.

Contribution of protein and glycan elements to the VRC-PG05 epitope				
Components	Area (Å^2)	Area breakdown (Å^2)		Percentage (%)
		Heavy chain	Light chain	
Glycan295	286	105	181	14
Glycan262	739	739	0	35
Glycan448	811	391	420	39
Subtotal by glycans	1836	1236	601	88
Peptide	251	95	156	12
Total area	2087			

Paratope of VRC-PG05 and contribution of different complementarity determining regions				
Region	Heavy chain		Light chain	
	Area (Å^2)	%	Area (Å^2)	%
Framework 1	9.3	0.6	64.3	3.8
CDR 1	123.9	7.4	271.6	16.1
Framework 2	0	0.0	23.3	1.4
CDR 2	173.5	10.3	87.8	5.2
Framework 3	40	2.4	0.0	0.0
CDR 3	724.4	43.0	164.8	9.8
Framework 4	0	0.0	0.0	0.0
Total paratope	1071.1	63.6	611.8	36.4

Table S6. Contributions of VRC-PG05 heavy and light chain paratope residues to the binding of HIV-1 glycans and amino acids. Related to Figure 3 and 6.

Heavy chain

Glycan epitope		Paratope surface area (Å^2)																								
		Frw 1	CDR H1						CDR H2										CDR H3							
Glycan	Moiety	2 V	28 P	30 N	31 R	32 D	33 W	52A M	53 D	57 K	58 D	59 Y	61 D	64 K	94 R	95 I	96 R	97 Q	99 S	100A Y	100B L	100C Q	100D W	100E Y	101 E	Subtotal
N262	NAG762																				35	1				36
	NAG763																		7		14	5	52			78
	MAN764																						28			28
	MAN765				37													29					33			99
	MAN766		6		23	16									10	3	15	22							5	101
	MAN767				4		2	17										16					42			82
	MAN770		1												23		22	0							19	66
	MAN771			2	39			21	15									3								80
N295	NAG795																		19							19
	MAN798																38								1	39
	MAN799	3													7		5								17	31
N448	NAG948																			25	29	21				76
	NAG949																			45		19		7		70
	MAN950																			30				5		35
	MAN951																			6						6
	MAN954																							3		3
	MAN955									5	39									2				14		60
	MAN956										22	7	4	36												70
Subtotal for glycan		3	7	2	103	16	2	38	15	5	61	7	4	36	40	3	81	72	26	108	79	45	155	29	42	978
gp120 peptide																				20	1	92				113
Total for glycan		978																								
Total for peptide		113																								
Total on heavy chain		1091																								

Light chain

Glycan epitope		Paratope surface area (Å^2)																			
		Frw 1	CDR L1								CDR L2					CDR L3				
Glycan	Moiety	1 D	2 I	27 Q	27D Y	27E R	27F P	28 N	29 N	30 R	49 H	50 W	54 R	55 E	56 S	92 F	93 F	94 L	Subtotal
N295	NAG795							4		13		15							32
	MAN797														11				11
	MAN798										21		2	26	28				77
	MAN799													14	21				35
N448	NAG948				24		13												37
	NAG949				19		5												25
	MAN950															3	20		23
	MAN951	3		15													25		43
	MAN952	40	1	25													19		85
	MAN954																4		4
	MAN955																22	29	51
	MAN956	1															18	31	50
Subtotal for glycan		44	1	40	43		19	4		13	21	15	2	40	60	3	109	60	474
gp120 peptide					10	28	69	17	17										142
Total for glycan		474																	
Total for peptide		142																	
Total on light chain		615																	

Table S7. Hydrogen bonds between HIV-1 gp120 glycans and VRC-PG05. Related to Figure 3 and 6.

Heavy chain

##	VRC-PG05	Distance [Å]	gp120 glycans
1	H:TRP100D[NE1]	2.74	G:NAG763[O3]
2	H:GLN97[NE2]	3.23	G:MAN765[O3]
3	H:ARG31[NH1]	3.02	G:MAN765[O4]
4	H:GLN97[N]	2.93	G:MAN766[O3]
5	H:GLN97[NE2]	2.91	G:MAN766[O4]
6	H:ARG94[NH2]	3.84	G:MAN766[O6]
7	H:ASP32[OD1]	2.68	G:MAN766[O6]
8	H:ARG94[NH2]	3.8	G:MAN770[O4]
9	H:ARG31[NE]	2.56	G:MAN771[O6]
10	H:ARG96[NH2]	3.44	G:MAN798[O4]
11	H:GLN100C[NE2]	3.88	G:NAG948[O3]
12	H:TYR100A[O]	3.03	G:NAG948[N2]
13	H:GLN100C[NE2]	2.73	G:NAG949[O6]
14	H:LYS64[NZ]	2.87	G:MAN956[O2]
15	H:LYS64[NZ]	2.79	G:MAN956[O3]

Light chain

##	VRC-PG05	Distance [Å]	gp120 glycans
1	L:SER56[N]	2.79	G:MAN798[O3]
2	L:TYR27D[OH]	3.71	G:NAG948[O4]
3	L:ASP1[N]	2.54	G:MAN952[O6]

Figure S1

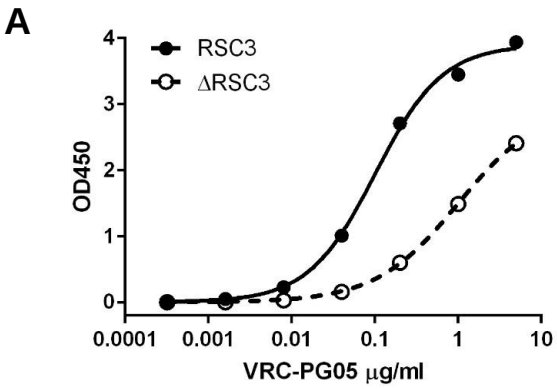

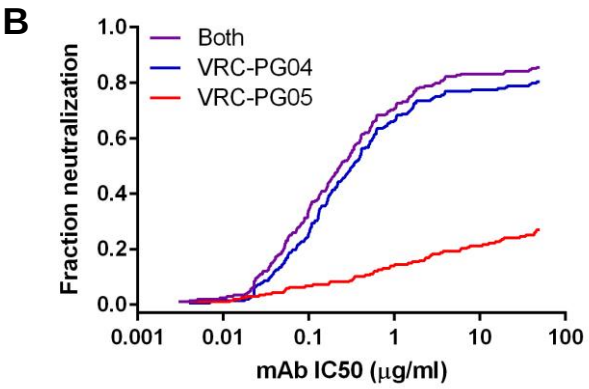

C

21-strains + AC10.29	Clade	Neutralization ID50/IC50 IAVI #74 plasma	VRC-PG04 μg/ml	VRC-PG05 μg/ml
BG505.W6M.C2	A	2591	0.041	>50
KER2018.11	A	507	0.167	>50
Q23.17	A	2967	0.050	>50
Q769.h5	A	5481	0.007	0.016
RW020.2	A	2862	0.100	>50
Q168.a2	AD	2297	0.059	>50
6101.10	B	272	0.204	43.5
BaL.01	B	2958	0.116	0.642
BG1168.01	B	118	1.05	>50
CAAN.A2	B	1340	1.66	0.003
JR-CSF	B	694	0.162	>50
JR-FL	B	4170	0.102	2.65
PVO.04	B	403	0.283	>50
THRO.18	B	<50	>50	>50
TRJO.58	B	213	0.020	>50
TRO.11	B	892	0.237	>50
Yu2	B	1133	0.063	>50
DU156.12	C	682	0.020	>50
DU422.01	C	273	>50	5.99
ZA012.29	C	1093	0.165	>50
ZM106.9	C	887	0.135	>50
AC10.29	*B*	*1863*	*>50*	*0.019*
Breadth (%)		21/22 (95%)	19/22 (86%)	7/22 (32%)
Potency (geometric mean)		1020	0.107	0.328

D

Donor	VRC01-like	b12-like	HJ16-like	8ANC195-like	PG9-like	PGT128-like	2F5-like	10E8-like	35O22-like	PGT151-like	VRC-PG05	Neut breadth (%)
IAVI #74	0.50		0.21						0.16		0.13	95%
704010581		0.34		0.27		0.38			0.01			100%
707010219	0.14		0.05	0.08	0.72							100%
703010401				0.33	0.54			0.12		0.02		100%
707010175		0.25		0.33	0.15	0.24		0.03				95%
707010457		0.34		0.66								95%
705010534		0.24			0.15	0.34				0.28		95%
706010383		0.05	0.41			0.15		0.22	0.18			95%
703010505	0.31	0.45	0.02							0.20		90%
707010562	0.51		0.24		0.08	0.14			0.02			90%
703011852		0.21		0.14		0.61		0.04				90%
702010440		0.34		0.29		0.33		0.04				90%
703010694	0.25	0.19				0.48			0.08			86%
703011749		0.32		0.25		0.43						86%
703011754	0.10	0.35			0.24	0.09	0.02			0.10	0.09	86%
703010547		0.16	0.18	0.19		0.45				0.02		86%
707010277	0.32	0.32	0.05	0.09				0.16			0.06	86%
700010111		0.29	0.14	0.35		0.16	0.03		0.03			86%
704010540	0.17	0.21	0.36	0.26								86%
702010293		0.43				0.57						81%
705010765		0.09		0.02	0.08	0.81						81%
702010432		0.02			0.23	0.52	0.08		0.15			81%
707010763		0.23		0.03	0.16	0.41	0.06	0.04		0.08		81%
707010585			0.01	0.02	0.17			0.55	0.24			81%
707010232			0.15		0.54		0.17		0.14			76%
704010343		0.37		0.19		0.44						76%
702010141	0.04		0.55	0.04	0.01	0.32				0.04		76%
703010848						0.82	0.03			0.07	0.06	71%
703011244		0.25				0.29	0.04	0.42				71%
703010269		0.17			0.16	0.46		0.21				71%
704010210		0.22				0.24		0.54				62%
704010461		0.20		0.47		0.34						62%
705010406		0.36			0.21	0.33	0.09	0.01				57%
703010010	0.10	0.28	0.01	0.27	0.24	0.10	0.01					57%
707010060	0.17	0.18	0.10		0.15	0.11	0.09		0.21			48%
705010741		0.28		0.14	0.25	0.19			0.14			48%
700010592				0.05	0.18	0.25		0.17	0.29	0.05		43%
702010047		0.39	0.26		0.08			0.26				38%
704010083		0.20	0.23			0.32				0.13	0.12	38%

Figure S1. Binding and neutralization of VRC-PG05 and its relevance in donor plasma. Related to Figure 1.

(A) Differential binding of VRC-PG05 to RSC3 and ΔRSC3, the epitope-specific molecular probes used to isolate single B cells.

(B) Neutralization profile of VRC-PG04, VRC-PG05 and their combination on 208 HIV-1 isolates. Breadth (y-axis) and potency (x-axis) are plotted for VRC-PG04, VRC-PG05, and their combination as calculated based on neutralization by individual antibodies.

(C) Neutralization ID50 of donor IAVI #74 plasma (shown as reciprocal dilution) and IC50 for antibody VRC-PG04 and antibody VRC-PG05 (shown as concentration) on AC10.29 as well as on a 21-strain panel (Georgiev et al., Science 2013) used for neutralization fingerprint calculation in (D). Three VRC-PG04-resistant strains are highlighted.

(D) Neutralization fingerprint analysis of donor plasma (rows) deconvoluted into component antibody specificities (columns), including the VRC-PG05 component specificity. For each donor, the predicted contribution to neutralization from each of 11 antibody specificities (colored labels) is shown, with values ranging from 0 (no contribution) to 1 (donor neutralization can be attributed to a single antibody specificity) and with color intensity proportional to magnitude of values. Donor IAVI #74 (top row) and 38 other HIV-1-infected donors from a CHAVI cohort (subsequent rows), which was previously analyzed (Pancera et al., Nature 2014), but without the VRC-PG05 specificity that we define here.

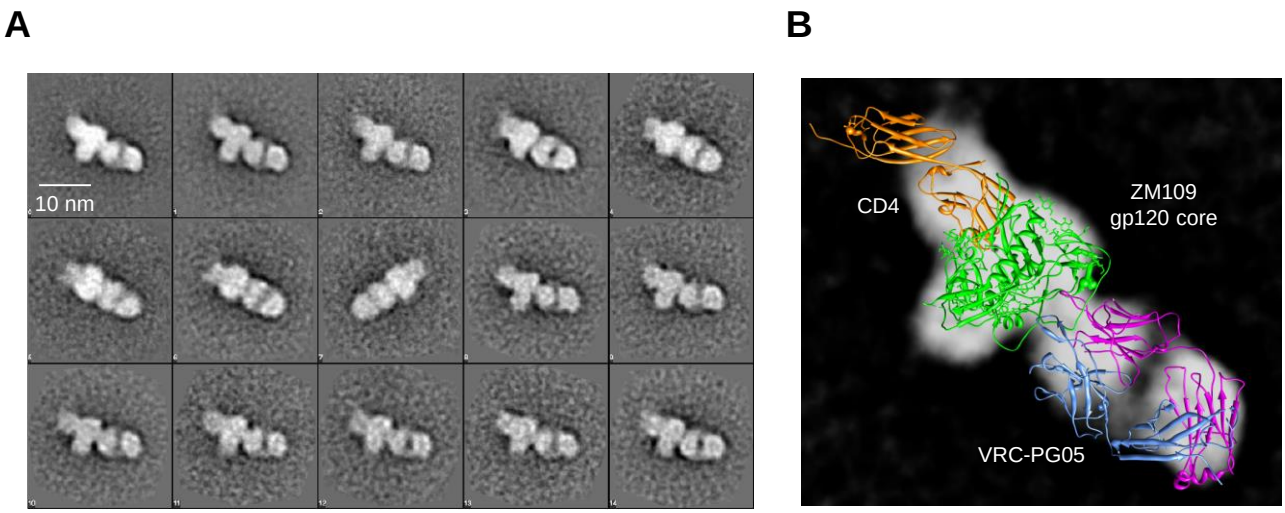

Figure S2. Negative-stain electron microscopy of VRC-PG05 bound to HIV-1 ZM109 gp120 core. related to Figure 2.

(A) Reference-free 2D classification of ternary complex of VRC-PG05, gp120 and two-domain CD4.

(B) Model of VRC-PG05, two-domain CD4 and gp120 were superposed onto the negative stain electron density.

Figure S3

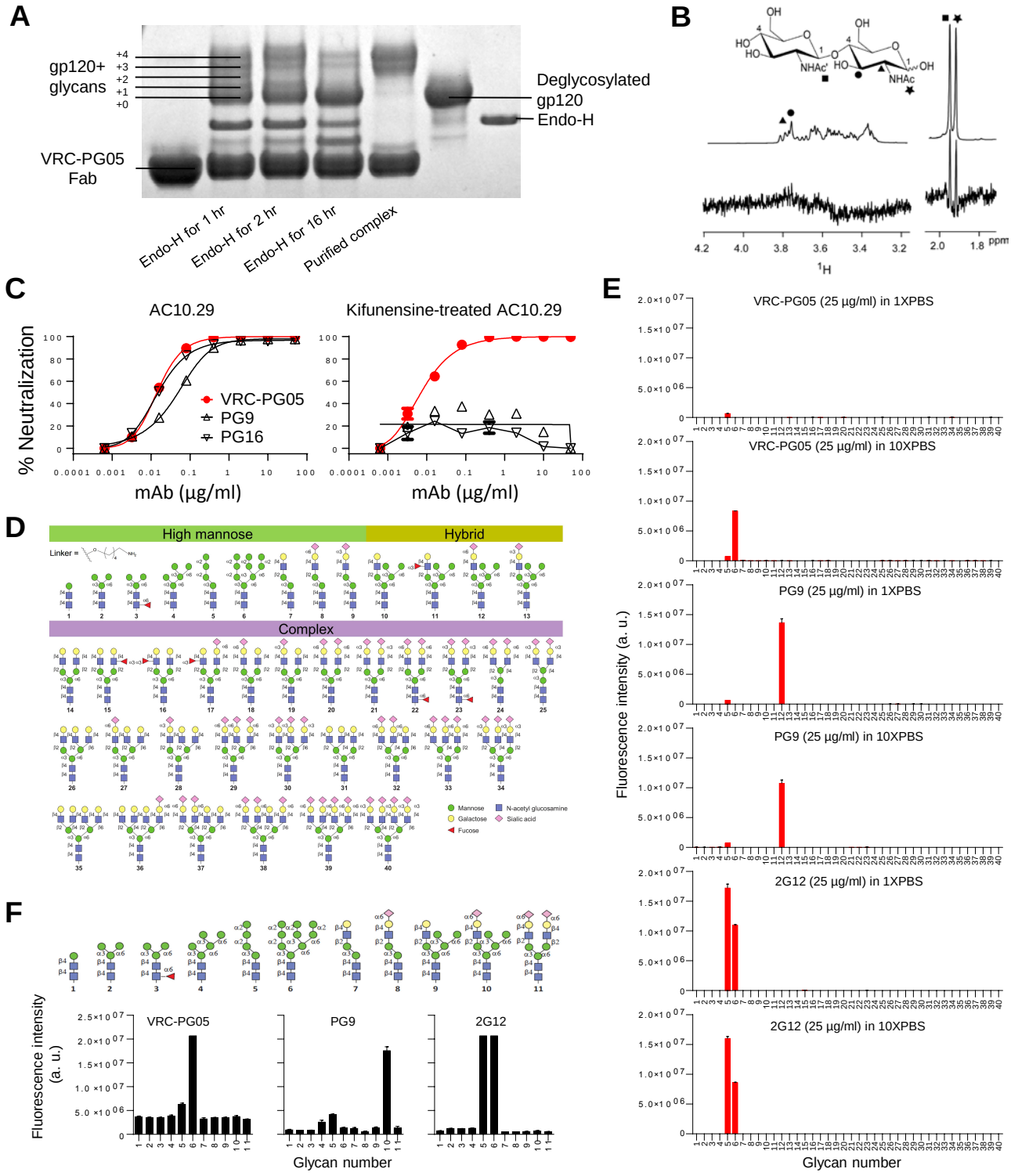

Figure S3. VRC-PG05 interaction with glycans. Related to Figure 3.

(A) Binding of VRC-PG05 shields several N-linked glycans on HIV-1 CNE55 gp120 from Endo-H digestion. SDS-PAGE analysis of samples at different time points of Endo-H digestion and the purified VRC-PG05-gp120 complex showed 3 to 4 glycans were protected by VRC-PG05.

(B) Nuclear magnetic resonance (NMR) analysis showed that VRC-PG05 binds to the two base N-acetylglucosamine groups at the N-linked glycosylation site.

(C) Neutralization of AC10.29 Env-pesudovirus generated in the presence of kifunensine indicates VRC-PG05 recognizes high mannose on gp120. Antibodies PG9 and PG16 were included as controls.

(D) Schematic representation of the 40 *N*-glycans printed on NHS-coated microarray glass slides.

(E) Binding profiles for antibodies VRC-PG05, PG9 and 2G12 to NHS-glycan array in 1x and 10x PBS; glycan numbers shown in (D).

(F) Schematic of the 11 *N*-glycans printed on ACG-coated microarray with binding profiles for antibodies VRC-PG05, PG9 and 2G12 in 1xPBS.

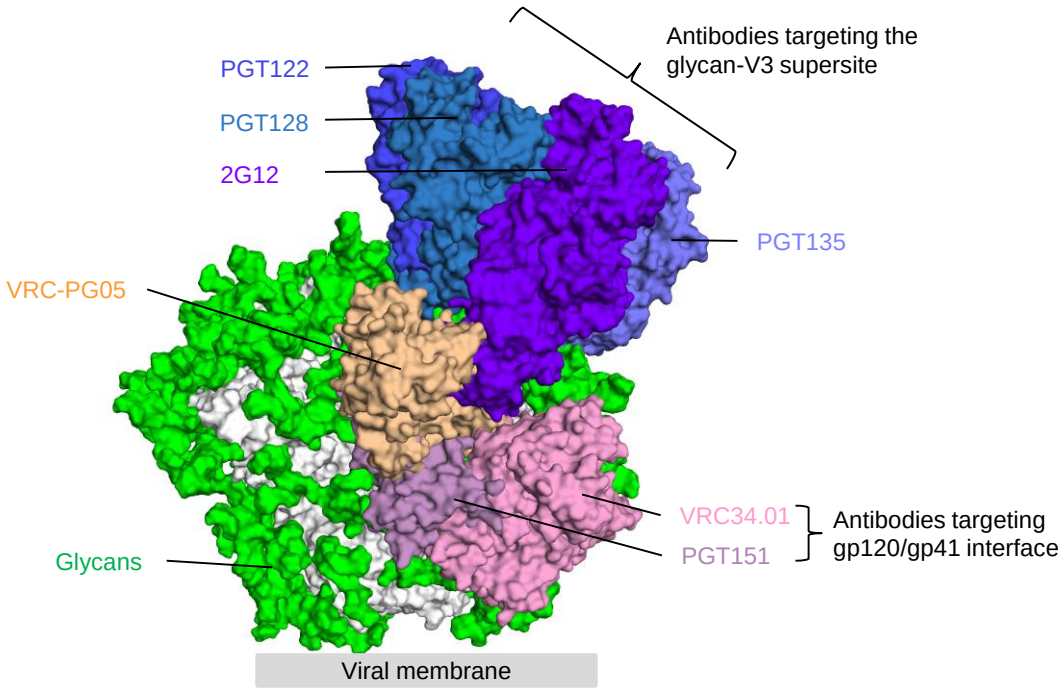

Figure S4. Comparison of modes of recognition of VRC-PG05 and other glycan-reactive antibodies. Related to Figure 4.

Binding modes and locations of VRCPG05 and antibodies targeting the glycan-V3 supersite and the gp120/gp41 interface . VRC-PG05 is colored in orange, glycan-V3 antibodies are shown in surface representation in shades of blue, and gp120/gp41 interface antibodies are colored in lavender/pink. HIV-1 Env is shown in gray surface with glycans shown in green.

Figure S5

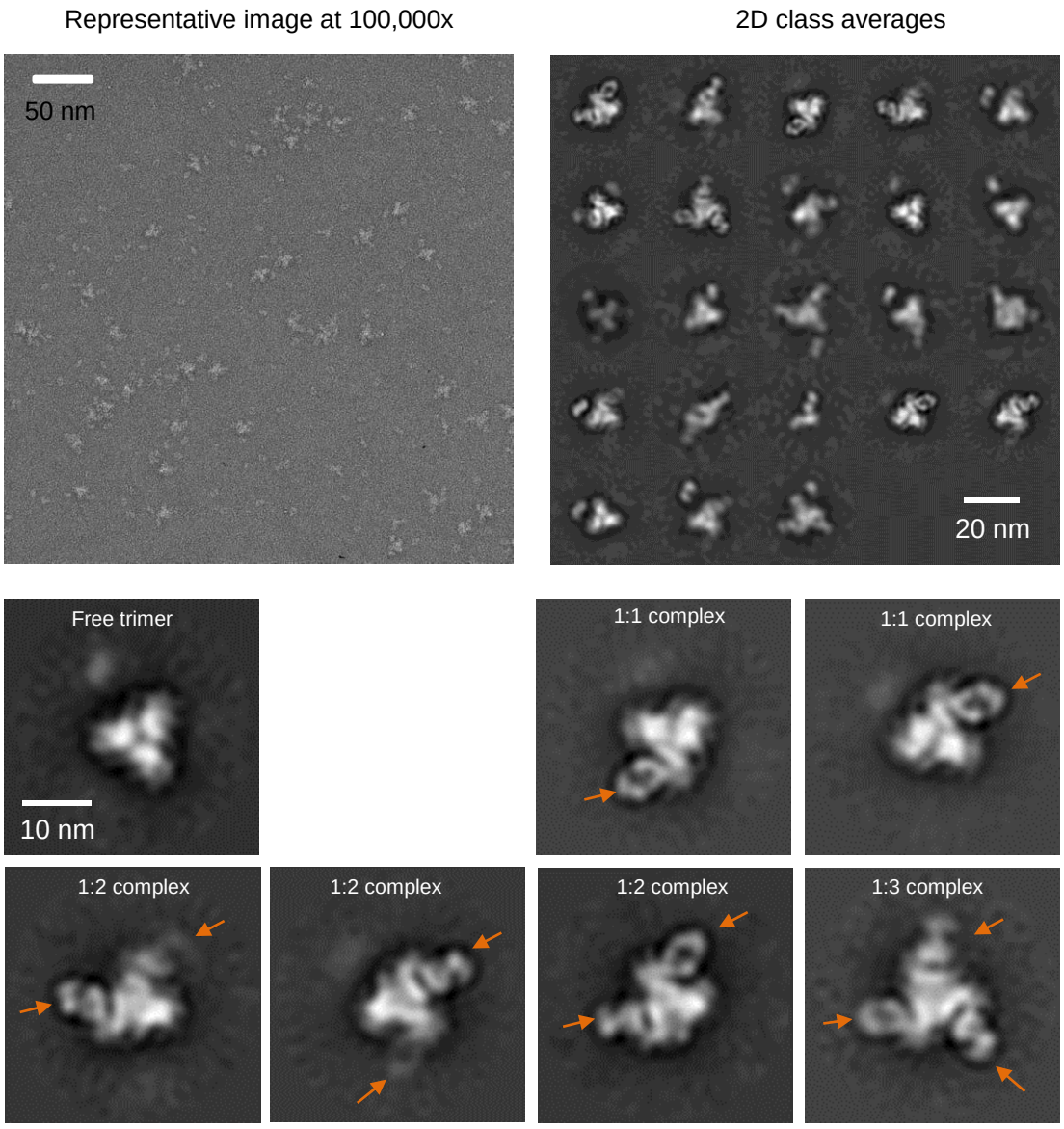

Figure S5. Negative-stain electron microscopy of AC10.29.SOSIP Env in complex with VRC-PG05. Related to Figure 5. Locations of VRC-PG05 Fab bound to Env trimer are marked by orange arrows. 1, 2 and 3 VRC-PG05 Fabs were observed to bind to each AV10.29 Env trimer.

Figure S6

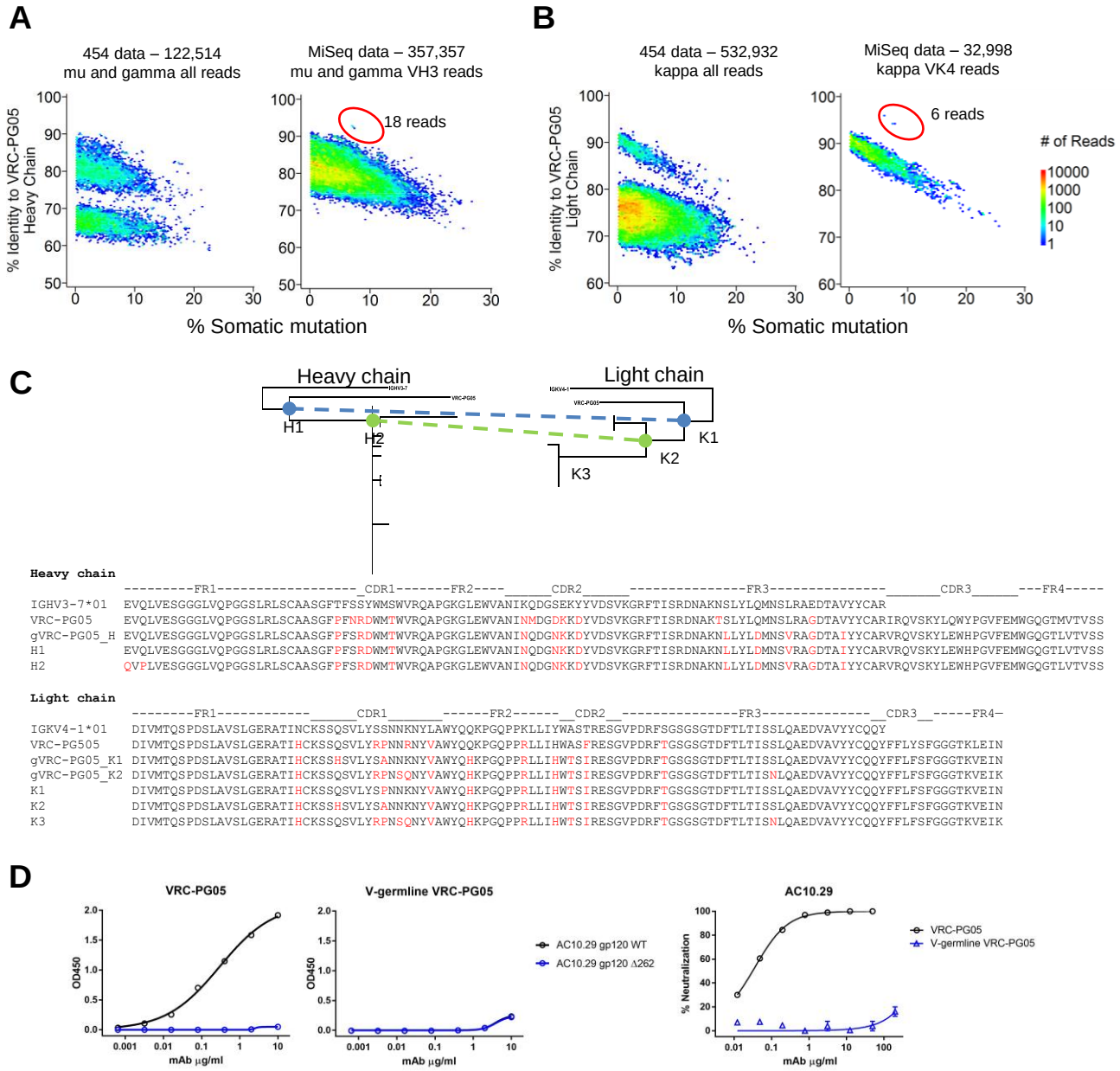

E

Somatic hypermutation in VRC-PG05 preferentially occurs at glycan contacts		
	SHM residues	Non-SHM residues
Glycan contacts	8*	17
Non-glycan contacts	13*	155

Figure S6. VRC-PG05 clonal variants identified by next generation sequencing. Related to Figure 6.
(A, B) Subsets of expressed heavy-chain (A) and kappa-chain (B) sequences obtained by NGS (454 data to left of MiSeq data) from IAVI donor #74 (2008 sample) are plotted as sequence identity to VRC-PG05 and sequence divergence from the putative germline V-genes. VRC-PG05 heavy and light chain variants derived from NGS are provided in (C) below each panel.
(C) Phylogenetic tree and inferred intermediate sequences of VRC-PG05 derived from NGS. Somatic hypermutations are colored red.
(D) Comparison of wild-type and V-gene-reverted VRC-PG05 by gp120 ELISA (left two panels) and neutralization (right panel) of strain AC10.29.
(E) Analysis of occurrence of somatic hypermutations in paratope of VRC-PG05. *P = 0.0017

Figure S7

A

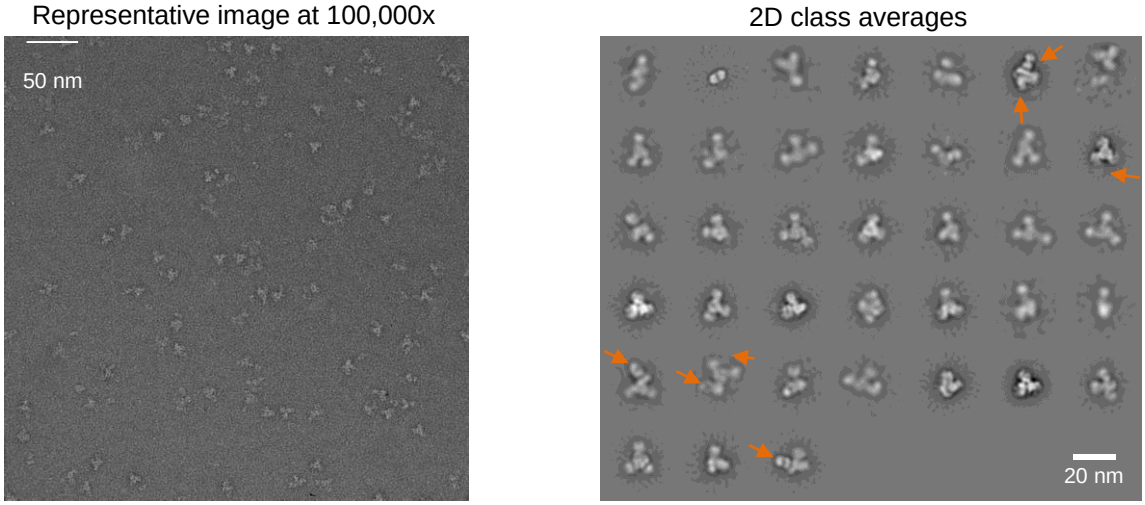

B

Donor #74 Env clones	VRC01	VRC-PG04	VRC-PG05	10E8
74_08dA06	>50	>50	>50	0.155
74_08dA13	>50	>50	21.7	0.897
74_08dA16	>50	>50	>50	0.496
74_08dA18	>50	>50	>50	0.441
74_08dB07	>50	>50	>50	1.160
74_08dB08	>50	>50	>50	1.930
74_08dB14	>50	>50	>50	1.150
74_08dB31	>50	>50	15.5	3.580

C

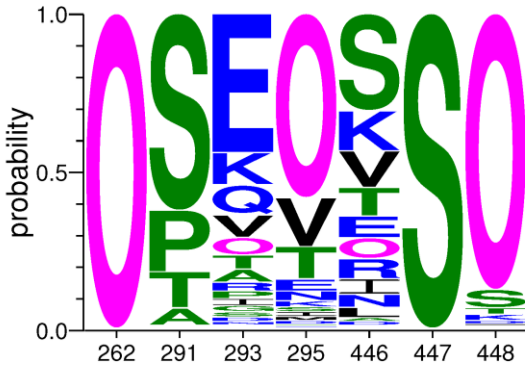

D

Position	Percentage and raw count of non-gap residues	Non-gap/total (percentage)	Gap/total (percentage)
262	O*: 99.52% (5139) other: 0.48% (25)	5164/5164 (100.00%)	0/5164 (0.00%)
291	S: 62.15% (3208) P: 19.51% (1007) T: 11.45% (591) A: 5.48% (283) other: 1.41% (73)	5162/5164 (99.96%)	2/5164 (0.04%)
293	E: 43.94% (2268) K: 10.17% (525) Q: 9.55% (493) V: 7.13% (368) O: 5.60% (289) T: 4.48% (231) A: 4.13% (213) R: 2.83% (146) P: 2.42% (125) I: 2.09% (108) G: 2.00% (103) S: 1.70% (88) other: 3.97% (205)	5162/5164 (99.96%)	2/5164 (0.04%)
295	O: 58.14% (3001) V: 15.56% (803) T: 10.25% (529) E: 3.84% (198) N: 3.08% (159) K: 1.96% (101) S: 1.61% (83) I: 1.36% (70) other: 4.22% (218)	5162/5164 (99.96%)	2/5164 (0.04%)
446	S: 30.75% (1587) K: 12.69% (655) V: 11.55% (596) T: 9.07% (468) E: 6.84% (353) O: 6.65% (343) R: 6.39% (330) I: 4.84% (250) N: 4.20% (217) L: 3.20% (165) other: 3.82% (197)	5161/5164 (99.94%)	3/5164 (0.06%)
447	S: 99.54% (5139) other: 0.46% (24)	5163/5164 (99.98%)	1/5164 (0.02%)
448	O: 87.24% (4504) S: 5.87% (303) T: 2.03% (105) other: 4.86% (251)	5163/5164 (99.98%)	1/5164 (0.02%)

* O: potential N-linked glycosylation site; other letters represents single-letter code for amino acids.

Figure S7. VRC-PG05 binding to BG505.SOSIP mutant, neutralization sensitivity of select autologous Env clones from IAVI donor #74 and sequence frequency analysis of epitope residues. Related to Figure 7.

(A) Negative-stain electron microscopy of BG505.SOSIP.Q393E in complex with VRC-PG05. Locations of bound-antibody were marked by orange arrows.

(B) Neutralization sensitivity of select autologous Env clones from a PBMC genomic DNA sample (02/05/2008) of IAVI donor #74.

(C) WebLogo plot of HIV-1 gp120 residues at positions 262, 291, 293, 446, 447 and 448 in 5164 sequences from the Los Alamos National Laboratory HIV database. Potential N-linked glycosylation site is represented by letter O, all amino acids are represented by single letter codes.

(D) Detailed list of amino acid frequency at each position.